WARSAW UNIVERSITY OF TECHNOLOGY Index 351733
FACULTY OF CIVIL ENGINEERING
COMMITTEE FOR CIVIL AND WATER ENGINEERING
POLISH ACADEMY OF SCIENCES ISSN 1230-2945
DOI: 10.24425/ace.2025.154141
ARCHIVES OF CIVIL ENGINEERING
Vol. LXXI ISSUE 2 2025
pp. 623–640

Research paper

Parameter analysis of a cable-stayed bridge without backstays

Xilong Zheng[1]

Abstract: A cable-stayed bridge without backstays is an important branch of the cable-stayed bridge family. It tilts the bridge tower to one side and removes the backstay cable, relying on its own weight to balance the tension in the slanted cables. It has the characteristics of novel structure and beautiful appearance and is highly favored in the construction of urban areas both domestically and internationally. This paper, based on the main bridge construction project of the Jinzhou Bridge, uses finite element analysis software to establish a spatial model and simulate the construction process, focusing on parameter analysis and the effect of bridge tower tilt angle. The paper analyzes the impact of changes in parameters such as structural stiffness and tension on the structure in the completed bridge state, and concludes that the sensitivity parameters affecting the deformation and internal force of the bridge are tension, temperature, and shrinkage creep, while the insensitivity parameter is structural stiffness. The force state of the cable-stayed bridge without backstays is closely related to the tilt angle of the tower. By changing the tower's tilt angle, the paper studies the changes in the structural forces and the impact of the tower tilt angle on the structural performance and bridge cost.

Keywords: cable-stayed bridge without backstays, parameter analysis, tilt angle, stiffness

[1]PhD., Harbin University, School of Intelligent and Architectural Engineering, No.109 Zhongxing Da Dao, Harbin, China, e-mail: sampson88@126.com, ORCID: 0000-0001-5571-667X

1. Introduction

The cable-stayed bridge is a type of bridge structure where the bridge deck is subjected to compression and the support system is subjected to tension. The bridge deck system consists of girders, while the support system is comprised of steel cables [1–4]. Its main characteristic is the utilization of inclined cables as elastic supports for the bridge span, reducing the sectional bending moment, decreasing the self-weight of the main girder, and enhancing the bridge's spanning capacity [5].

Since the 1990s, with the development of cable-stayed bridge construction technology worldwide, China's cable-stayed bridges have embraced new opportunities and prospects. Several large-span cable-stayed bridges with spans exceeding 500 m have been constructed, such as the representative Nanpu Bridge and Yangpu Bridge in Shanghai [6,8]. These projects have fostered numerous talents in bridge design and construction, accumulating valuable construction experience and technology. Subsequently, a series of kilometer-level cable-stayed bridges with world-leading standards were constructed. Through decades of hard work and independent innovation, China's cable-stayed bridge construction has been advancing toward the world's top level [9,10].

In the continuous development of cable-stayed bridges, researchers have discovered through studies on backstay cable cable-stayed bridges that it is possible to increase the inclination angle of the main tower, eliminate the backstay cables on the backside of the tower, and ultimately form a unique and novel structural form known as a backstay-free cable-stayed bridge [11,12]. This involves removing the inclined cables on one side of the single tower cable-stayed bridge and tilting the tower towards that side to balance the tension of the inclined cables with its own weight. This bridge design has a visually striking impact, attracting the attention of the public. Once constructed, it becomes a representative architectural landmark of the city and is favored by designers and local governments [13]. However, this bridge design is not widely constructed around the world. The reasons for this are primarily due to the complex stress state of the bridge, which requires consideration of multiple factors, and limited efforts in related design work. Additionally, the unique structural form of this bridge design poses greater difficulties in construction compared to conventional cable-stayed bridges of similar spans [14].

Currently, there are only a dozen or so backstay-free cable-stayed bridges in the world that have been put into use, and the majority of them are pedestrian bridges. China has constructed several backstay-free cable-stayed bridges, including the Sun Bridge (the first backstay-free cable-stayed bridge in Asia) and Tongling Road Bridge in Hefei. Due to its aesthetic appeal and cost-effectiveness, backstay-free cable-stayed bridges have been increasingly favored by designers, leading to an increase in construction projects [15]. In view of this situation, it is necessary to conduct in-depth research on the construction control and parameter analysis of backstay-free cable-stayed bridges, draw useful conclusions, and address the problems encountered in the construction of such bridges, providing reference for design and construction decisions.

2. Engineering background

The main bridge of Jinzhou Bridge in Dalian, Liaoning Province, is a single-tower, single-cable-surface cable-stayed bridge with a fixed system of piers, towers, and beams. The maximum longitudinal slope of the bridge deck is 1.38%, and the main span is on a convex

vertical curve with a radius of 14,000 m. The cable tower adopts drilled pile foundation and a single-column inclined steel-reinforced concrete tower with a variable rectangular cross-section. The height of the cable tower is 124.2 m.

The main beam adopts a steel-concrete composite box girder with a concrete bridge deck on its top. The beam has a height of 3.0 m at the centerline and a full width of 30.5 m. The bridge deck has a 2% bidirectional cross slope. The inclined tension cables use finished parallel steel wires with a PE protective cover. The elevation of the Jinzhou Bridge main bridge is shown in Fig. 1.

Fig. 1. Elevation drawing of the main bridge of Jinzhou bridge

1. Cable tower

The cable tower adopts a single-column concrete inclined tower with a horizontal inclination angle of 55° and a rearward inclination angle of 35°. The rearward inclination angle of the tower is the largest among similar types of bridges. The total height of the cable tower is 124.2 m. The lower part of the cable tower has a variable box-shaped cross-section, with dimensions ranging from 24.574×5.142 m to 16.509×3.5 m. The upper part of the cable tower has a variable rectangular cross-section, with dimensions ranging from 10.862×4.5 m to 5.0×4.5 m.

2. Main beam

The main beam of this bridge is divided into concrete box girder and steel-concrete composite box girder. The concrete box girder is the main beam at the junction of pier, tower, and beam, with a length of 10.0 m and a central beam height of 3.0 m, as shown in Fig. 2 in cross-section. The steel-concrete composite box girder has a central beam height of 3 m. The top slab of the box girder is made of C50 polypropylene fiber concrete, while the bottom slab and web plates are made of steel. The steel-concrete composite beam has a top width of 30.5 m, a bottom width of 10.0 m, and the cross-section of main beam near tower is shown in Fig. 3. The cross-section of main beam is shown in Fig. 4. It adopts a three-box structure with cantilever beams set on the outer sides, with a longitudinal spacing of 4.0 m. The top surface of the box girder's top slab has the same cross slope as the alignment slope.

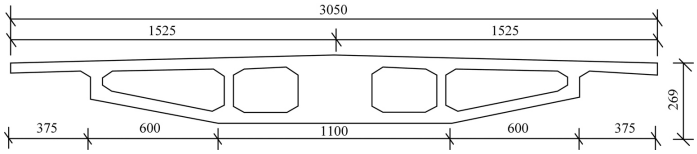

Fig. 2. Cross-sectional diagram of the main bridge of Jinzhou Bridge (1) (mm)

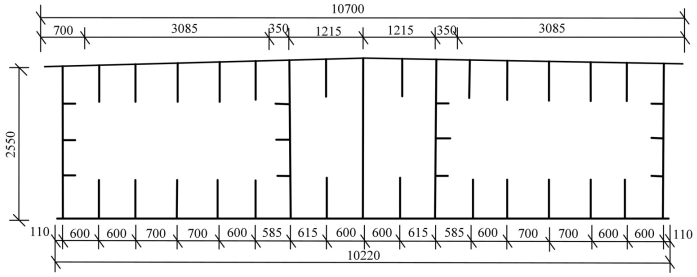

Fig. 3. Cross-sectional diagram of the main bridge of Jinzhou Bridge (2) (mm)

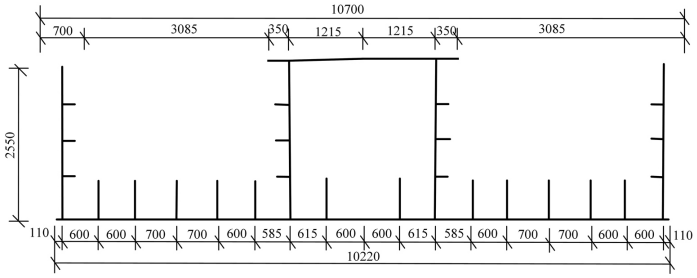

Fig. 4. Cross-sectional diagram of the main bridge of Jinzhou Bridge (3) (mm)

The steel beams are fabricated in segment lengths of 4 m, 5 m, and 6 m respectively. The steel beams are assembled on-site after being manufactured in the factory. The steel box girder is equipped with transverse partitions and longitudinal stiffeners. The bottom plate of the steel box girder is 24 mm thick, the wing plate is 20 mm thick, the inner web plate is 30 mm thick, and the transverse partition is 20 mm thick.

3. Cable tower

The cables are arranged in a harp shape, with a horizontal spacing of 1.6 m between cable anchoring points on the beam. The standard cable spacing for diagonal cables on the main beam is 12.0 m, and the first pair of cables extend to 22.0 m at the tower intersection. There are three types of cables, with 6 of each type, for a total of 18 cables. The longest cable is 196.055 m, and the shortest is 44.732 m. Fixed-end anchorages are used at the cable towers, and tensioning-end anchorages are used within the main beam. Anchor blocks are installed on the tower to anchor the cables, and pre-embedded anchor pipe and anchor plates are used. Steel anchor boxes are used to connect the main beam.

3. Structural analysis model establishment

The modeling and analysis of the main bridge of Jinzhou Bridge are performed using the Midas/Civil finite element analysis software. A spatial truss system model is established. According to the calculation method of finite element analysis, before building the model, the structure needs to be discretized. The discretization should follow certain principles. Otherwise, the built model will either require excessive computation time for the same level of accuracy or have significant discrepancies in the stress distribution compared to the actual structure. In this study, for computational convenience and considering the construction sequence, the structure is divided into 262 units. The division of the entire bridge units is shown in Fig. 5. Bridge pier, bridge tower and main beam are simulated by beam element, and cable is simulated by truss element. The pier bottom is consolidated.

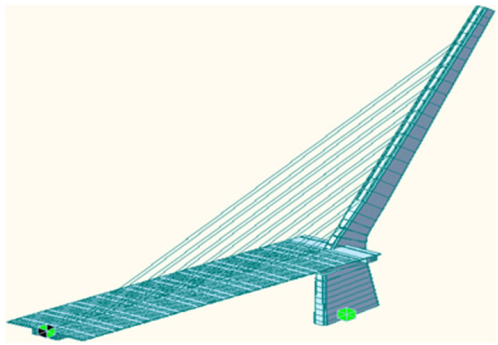

Fig. 5. Finite element discretization diagram of the structure

When simulating the main beam, the stiffness (torsional stiffness, lateral bending stiffness, and vertical bending stiffness) and mass of the main beam are all concentrated on the central axis of the main beam. The constraints on the main beam at the pier are modeled using general supports that constrain the horizontal lateral displacement D_y, vertical displacement D_z, and rotation around the z-axis R_z, based on the actual types of supports set.

4. Parameter sensitivity analysis

4.1. Impact of main beam stiffness error

The main beam of this bridge adopts a steel-concrete composite structure, and the stiffness of the main beam is influenced by both concrete and steel materials. During the pouring process of concrete, the elastic modulus may have errors due to the influence of construction techniques and construction temperature. Similarly, during the manufacturing and processing of steel, errors can occur during the smelting and forging processes. In this study, the influence of main beam stiffness is analyzed under four scenarios: increase by 2%, increase by 5%, decrease by 2%, and decrease by 5%. The analysis aims to assess the impact of main beam stiffness on the overall structural linearity and internal force state.

During the analysis of the impact of main beam stiffness, the actual errors are simulated by adjusting the elastic modulus of the materials. Based on this, the influence on the horizontal displacement of the cable tower, the nodal displacement of the main beam, the tension of the inclined cables, and the stresses in the main beam can be calculated for the as-constructed state. Please refer to Fig. 6–10 for the corresponding results.

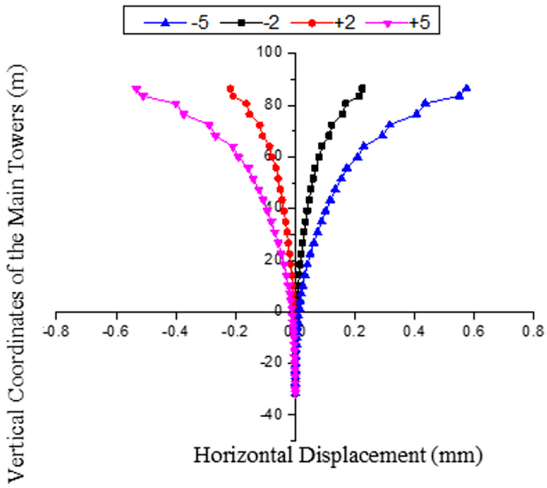

Fig. 6. Change in horizontal displacement of the stay tower after the stiffness modification of the main beam

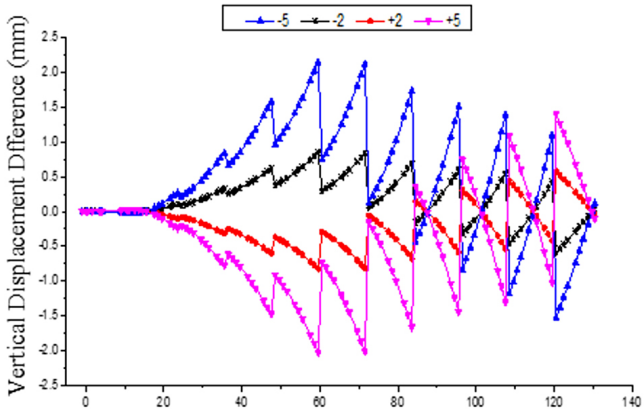

Fig. 7. Vertical displacement change of the main beam nodes after the stiffness modification of the main beam

According to Fig. 6, it can be observed that the horizontal displacement of the bridge tower varies within the range of −0.6 mm to 0.6 mm when the stiffness of the main beam is increased or decreased by 5%. This indicates that the stiffness of the main beam has a minimal impact on the horizontal displacement of the bridge tower.

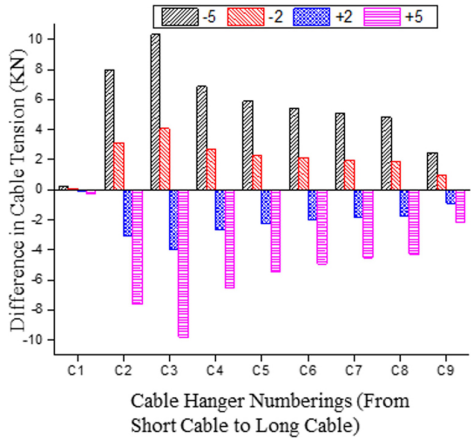

Fig. 8. Change in tension force of the inclined cables after the stiffness modification of the main beam

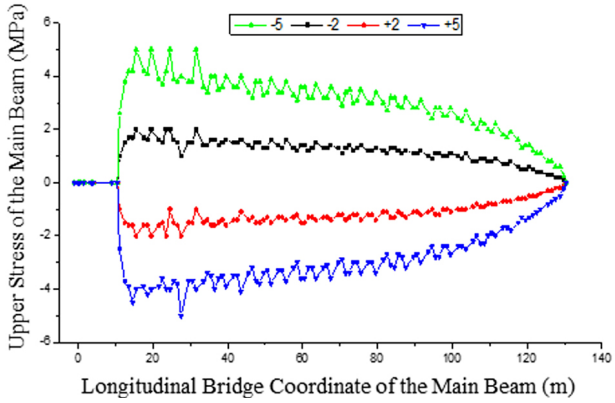

Fig. 9. Change in stress of the upper flange of the main beam after the stiffness modification

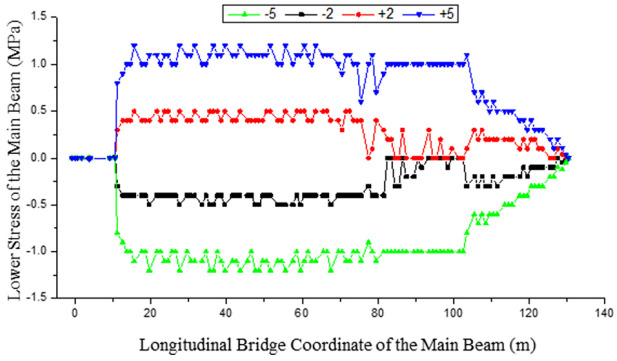

Fig. 10. Change in stress of the lower flange of the main beam after the stiffness modification

According to Fig. 7, it can be seen that the vertical displacement of the main beam varies between −2.1 mm and 2.0 mm when the stiffness of the main beam increases or decreases by 5%. In addition, the variation of the vertical displacement of the main beam increases with the increase of the stiffness error. Therefore, it can be concluded that the effect of stiffness on the vertical displacement of the main beam is relatively small.

According to Fig. 8, it can be observed that the variation of cable force increases with the increase of stiffness error in the main beam. At a certain stiffness state, the increment of cable force gradually increases from the bridge tower towards the abutment, and then decreases after passing through cable C3. In different stiffness states, the influence of the side cable near the bridge tower is relatively small, while the influence of other cables is significant. When the stiffness of the main beam increases by 5%, cable C8 shows the highest rate of force increase at 0.05%, indicating that the effect of main beam stiffness on cable force is minimal.

According to Fig. 9 and Fig. 10, it can be seen that the influence of main beam stiffness on the stress of the concrete main beam is relatively small, with a maximum variation of 0.01 MPa. However, the stress variation of the steel box girder increases with the increase of stiffness error in the main beam, and the value gradually decreases from the bridge tower towards the abutment in the longitudinal position. Within the range of increasing or decreasing 5%, the upper edge stress varies between −5.0 MPa and 5.0 MPa, and the lower edge stress varies between −1.2 MPa and 1.2 MPa, indicating that the effect of main beam stiffness on the stress of the main beam is minimal.

4.2. The influence of stiffness error of the cable-stayed bridge

The main reason for the stiffness error in the cable-stayed bridge lies in the elastic modulus E and cross-sectional area A of the steel strands that make up the cables. The steel strands are manufactured in factories with precise dimensions, thus their influence on E and A is minimal. During the process of bundling the cables, the tightness and coordination of the bundled cables may be affected, leading to a disparity in sag effects. The presence of HDPE sheaths restricts the free sag of the cables, resulting in errors in their axial stiffness. This study considers four scenarios: increasing the cable stiffness by 2% and 5%, decreasing the cable stiffness by 2% and 5%, and analyzes the degree of influence on the structural geometry and internal force state. The results are shown in Fig. 11–15.

According to Fig. 11, it can be observed that the horizontal displacement of the bridge tower varies between −0.26 mm and 0.24 mm when the cable stiffness changes by 5%. This suggests that the change in cable stiffness has a minimal effect on the horizontal displacement of the bridge tower.

Based on Fig. 12, it can be observed that the vertical displacement of the main beam varies between −14.7 mm and 15.8 mm when the cable stiffness changes by 5%. The vertical displacement of the main beam increases with the increase in cable stiffness error, indicating that the cable stiffness has a relatively small effect on the vertical displacement of the main beam.

Based on Fig. 13, it can be observed that the cable force of the inclined cable increases with the increase in cable stiffness error. At a certain stiffness state, the incremental force gradually increases from the bridge tower towards the abutment, reaching a peak at the C2 cable. After

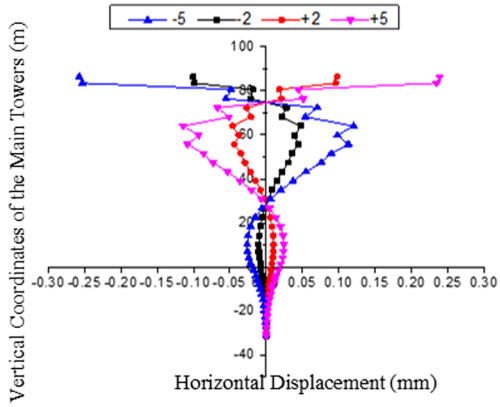

Fig. 11. The change in cable stiffness affects the horizontal displacement of the pylons

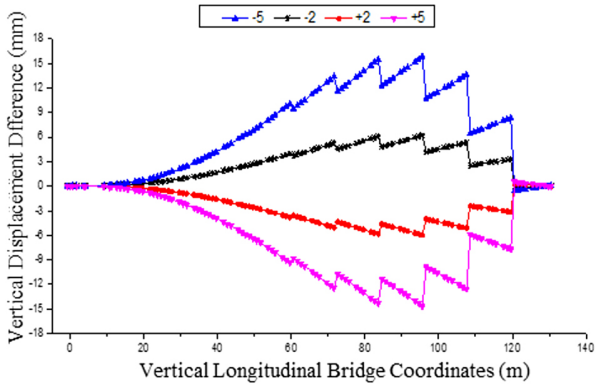

Fig. 12. After the change in cable stiffness, there will be variations in the vertical displacement of the main beam nodes

passing through the C3 cable, the sign of the increment changes, reaching a peak at the C8 cable, and then decreases. Among different stiffness states, the influence on the C4 cable is relatively small, while the influence on the remaining cables is significant. When the cable stiffness increases by 5%, the C8 cable exhibits the highest growth rate of −0.12%, indicating that cable stiffness has a minimal effect on cable forces.

Based on Fig. 14 and Fig. 15, it can be observed that the influence of cable stiffness on the stress of the concrete main beam is relatively small, with a maximum variation of 0.01 MPa. The stress variation of the steel box beam increases with the increase in cable stiffness error, and the values gradually decrease from the bridge tower to the abutment in the longitudinal position. Within the range of ±5% variation, the upper surface stress varies between −1.0 MPa and 1.0 MPa, while the lower surface stress varies between −3.1 MPa and 3.4 MPa. This suggests that cable stiffness has a minimal effect on the stress of the main beam.

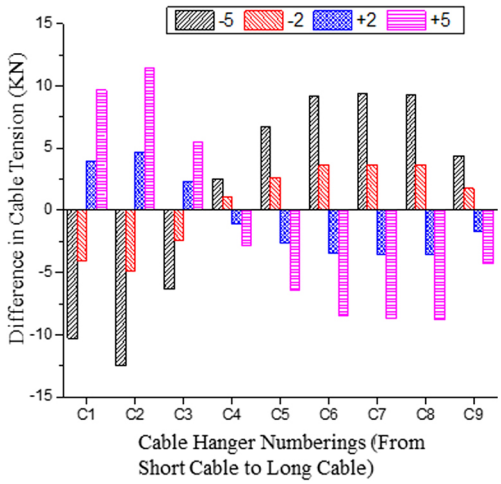

Fig. 13. The change in cable stiffness results in variations in the cable tension

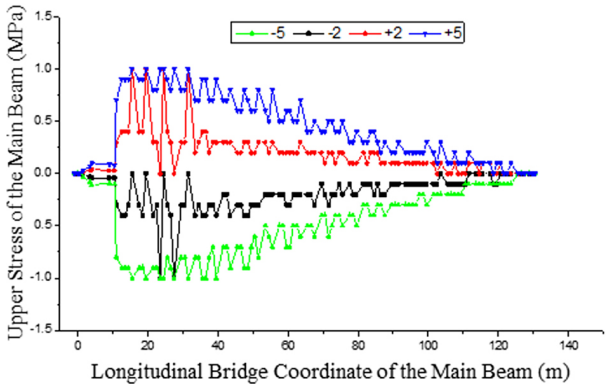

Fig. 14. The change in cable stiffness leads to variations in the stress of the upper edge of the main beam

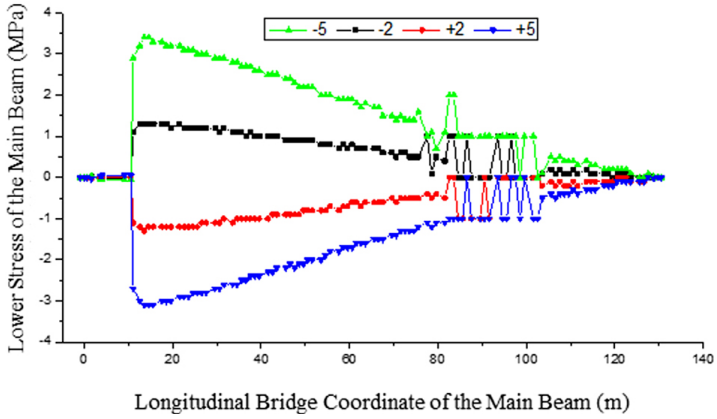

Fig. 15. The change in cable stiffness can cause variations in the stress of the lower edge of the main beam

4.3. Analysis of the impact of cable tensioning error on cable-stayed bridges

This study considers four situations regarding cable tensioning errors: an increase of 2%, an increase of 5%, a decrease of 2%, and a decrease of 5%. Based on these scenarios, the analysis examines the extent of the impact on the horizontal displacement of the cable tower, nodal displacement of the main beam, cable tension, tower stress, and main beam stress in the completed bridge state. The results are presented in Fig. 16–22.

According to Fig. 16, it can be seen that when the cable tension increases or decreases by 5%, the horizontal displacement of the cable tower ranges from −9.4 mm to 9.4 mm. The magnitude of horizontal displacement of the cable tower increases with the increase of cable tension error. At the position with the vertical coordinate of 81 m (location of cable C7), the cable tower exhibits the maximum horizontal displacement. With a 2% increase in cable tension, the displacement increment is 3.8 mm, while with a 5% increase in cable tension, the displacement increment is 9.4 mm, causing the cable tower to shift towards the abutment. When the cable tension increases or decreases by the same percentage, the horizontal displacement change of the cable tower remains virtually the same, indicating that cable tension errors have a symmetric influence on the horizontal displacement of the cable tower.

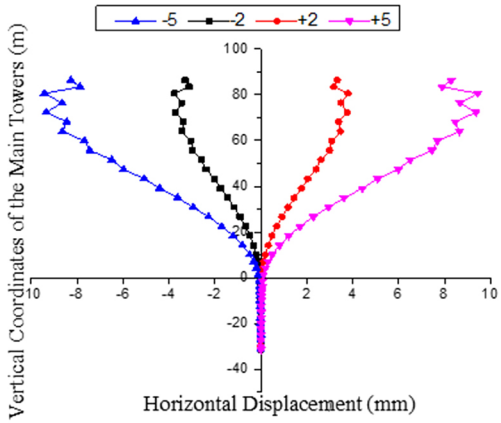

Fig. 16. Change in horizontal displacement of the cable tower after a change in cable tension

Based on Fig. 17, it can be observed that when the cable tension increases or decreases by 5%, the vertical displacement of the main beam ranges from −127.0 mm to 127.0 mm. The magnitude of vertical displacement of the main beam increases with the increase of cable tension error. Cable tension errors have a significant impact on the vertical displacement of the main beam. According to the position of displacement change shown in the figure, it can be seen that the main beam exhibits significant changes at the location with a longitudinal bridge coordinate of 84 m (location of cable C6). With a 2% increase in cable tension, the displacement increment is 50.8 mm, while with a 5% increase in cable tension, the displacement increment is 127.0 mm, causing the main beam to undergo an upward displacement. The displacement

increment of the main beam gradually increases from the bridge tower towards the abutment, reaches a peak at C6, and then gradually decreases. The displacement change in the cable-free zone near the bridge tower and abutment is relatively small, while the displacement change in the cable-supported zone is significant.

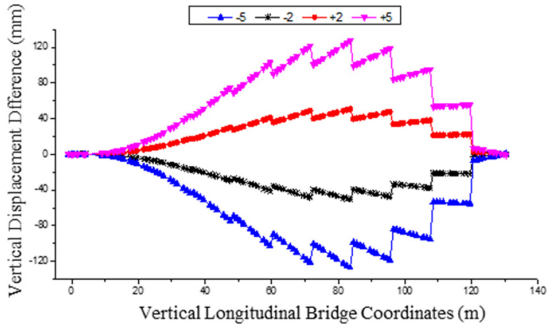

Fig. 17. Change in vertical displacement of the main beam node after a change in cable tension

Based on Fig. 18, it can be observed that the cable tension of the stay cables increases with the increase of cable tension error. At a certain error state, the increment of cable tension gradually decreases from the bridge tower towards the abutment. When the cable tension increases by 5%, the cable tension growth rate of cable C1 is the highest at 4.7%, while the cable tension growth rate of cable C6 is the lowest at 2.4%. This indicates that cable tension errors have a significant impact on the cable tensions in the completed bridge state.

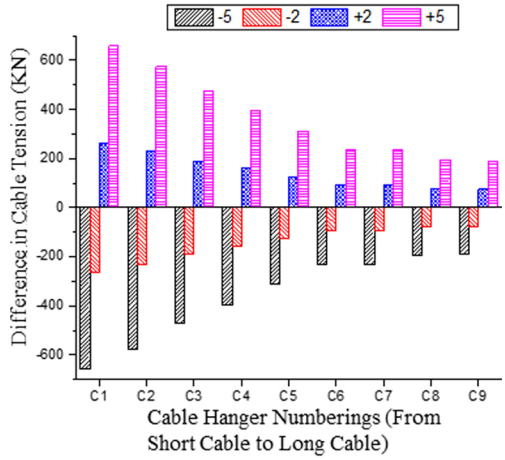

Fig. 18. Change in cable tension of the inclined cable after a change in cable tension

Based on Fig. 19 and Fig. 20, it is evident that cable tension errors have a significant impact on the stress of the concrete main beam. The maximum variation is −1.94 MPa. At a cable tension error of 2%, the upper surface stress of the concrete changes by −0.77 MPa, while at

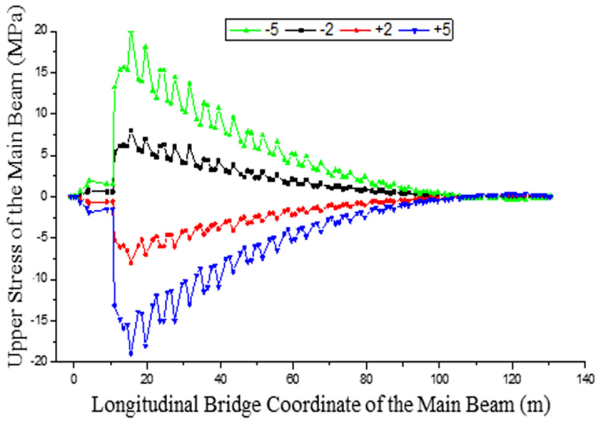

Fig. 19. Change in stress on the upper surface of the main beam after a change in cable tension

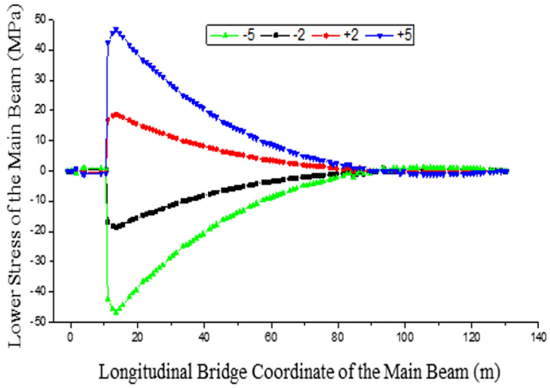

Fig. 20. The stress on the lower edge of the main beam changes after the change in cable tension

a cable tension error of 5%, the upper surface stress of the concrete changes by −1.93 MPa, resulting in an increase in compressive stress on the upper surface and an increase in tensile stress on the lower surface. The stress variation of the steel box girder increases with the increasing cable tension error of the stay cables, with the values gradually decreasing from the bridge tower towards the abutment in the longitudinal direction. Within the range of a 5% increase or decrease in cable tension, the upper surface stress varies between −19.0 MPa and 20.1 MPa, and the lower surface stress varies between −46.8 MPa and 46.8 MPa, demonstrating the significant influence of cable tension errors on the stress of the main beam. The upper and lower surface stresses of the steel box girder exhibit larger variations in the first half of the bridge and gradually decrease in the second half. This indicates that the sensitivity of the upper and lower surface stresses of the steel box girder to cable tension is greater in the first half, and smaller in the second half.

Based on Fig. 21 and Fig. 22, it can be observed that the stress variations on the left and right sides of the bridge tower increase with the increase of cable tension errors. When the cable tension errors increase or decrease by 5%, the compressive stress on the cable-free side of the bridge tower (the left side) decreases with a maximum decrement of 0.5 MPa. On the other side of the bridge tower (the right side), the tensile stress decreases and the compressive stress increases, with a maximum variation of −0.9 MPa for the compressive stress. From the range of variations, it can be concluded that cable tension errors have a relatively small impact on the stress of the bridge tower cross-section.

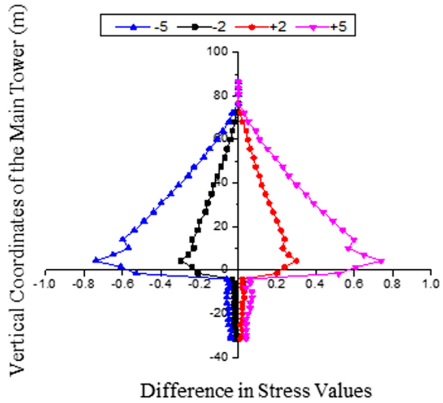

Fig. 21. The stress on the left side of the cable tower changes after the change in cable tension

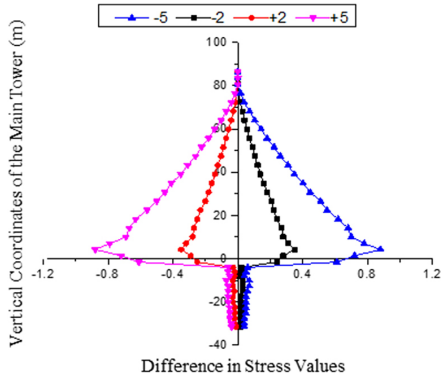

Fig. 22. The stress on the right side of the cable tower changes after the change in cable tension

4.4. Analysis of overall temperature difference impact

Simulations were conducted for four scenarios considering the overall temperature difference: a temperature increase of 10° and 20°, and a temperature decrease of 10° and 20°. The simulations were used to determine the impact of the overall temperature difference on the structure. The calculated values include the vertical displacement, stress, and cable tension variations in the bridge state, as shown in Fig. 23–27.

According to Fig. 23, it can be seen that the horizontal displacement variation of the tower caused by a temperature increase of 20°C and a temperature decrease of 20°C has reached −12.6 mm to 12.6 mm. The horizontal displacement variation of the tower increases with the increase of the temperature difference. The maximum horizontal displacement occurs at the top of the tower. For a temperature increase of 10°C, the displacement increment is −6.1 mm, while for a temperature increase of 20°C, the displacement increment is −12.6 mm, causing the tower to shift away from the pier. When the overall temperature increase and decrease are of the same percentage, the horizontal displacement variation of the tower is the same, indicating that the overall temperature difference has a symmetrical effect on the horizontal displacement of the tower.

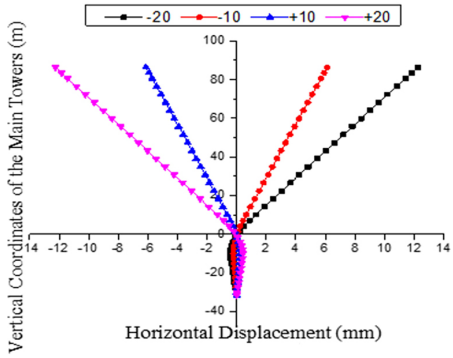

Fig. 23. Effects of overall temperature difference on horizontal displacement of the pylon

According to Fig. 24, it can be observed that when the structure undergoes an overall temperature increase of 20°C, it causes an upward deflection in the main beam near the tower root, with a maximum increment of 6.1 mm. The vertical displacement variation of the main beam increases with the increase of the temperature difference, but the overall temperature difference has a minimal effect on the vertical displacement of the main beam. During the temperature increase, the displacement increment of the main beam decreases gradually from the bridge tower to the abutment. At location C4, the main beam undergoes a downward deflection, with a maximum displacement of −3.4 mm.

According to Fig. 25, it can be seen that the tension force in the stay cables increases with the increase of the temperature difference. Under different temperature differences, the variation trend of the tension force is the same, with the increment of the tension force gradually decreasing from the bridge tower to the abutment. The stay cables numbered C1 to C3 have a significant impact, while the other cables have a smaller impact.

Based on Fig. 26 and Fig. 27, it can be concluded that the temperature difference has a significant impact on the stress of the concrete main beam at the tower root, with a maximum variation of −8.5 MPa. When there is a temperature increase of 10°C, the maximum variation in the upper part stress of the concrete is −4.2 MPa, while with a temperature increase of 20°C, the maximum variation in the upper part stress of the concrete is −8.5 MPa, causing an increase in compressive stress in the upper part. The stress variation in the steel box girder increases

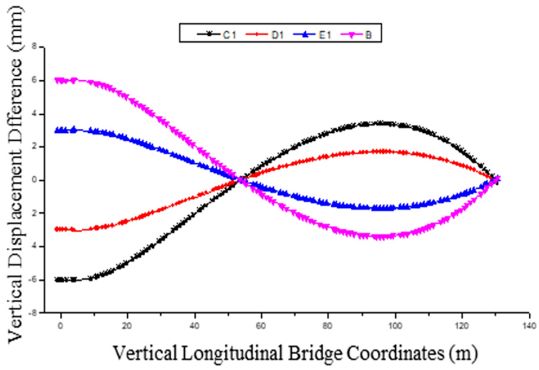

Fig. 24. Effects of overall temperature difference on vertical displacement of the main beam nodes

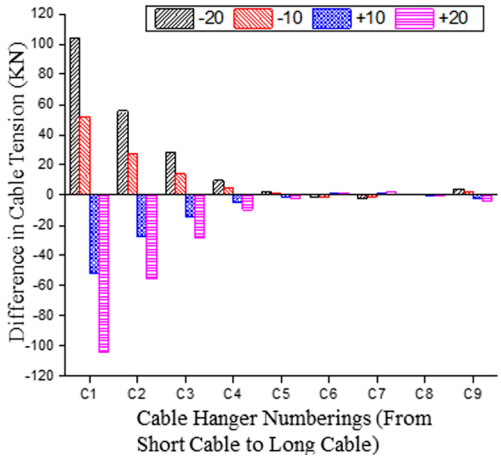

Fig. 25. Effects of overall temperature difference on cable tension variation of the stay cables

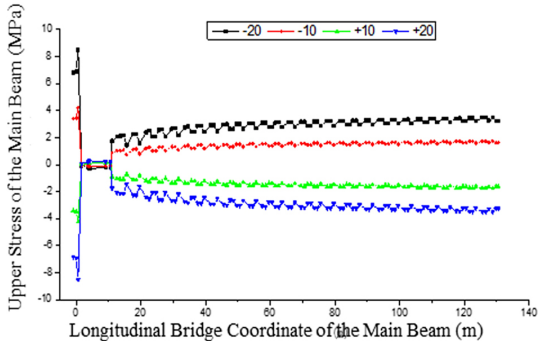

Fig. 26. Effects of overall temperature difference on stress variation in the upper flange of the main beam

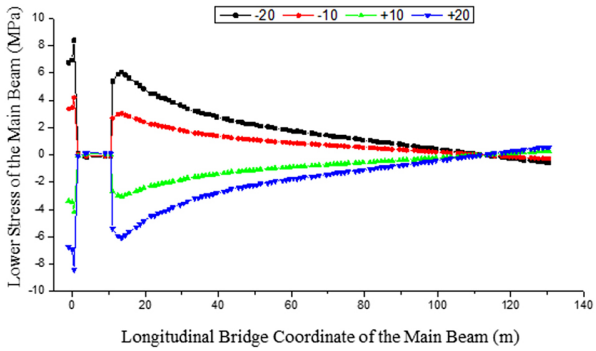

Fig. 27. Effects of overall temperature difference on stress variation in the lower flange of the main beam

with the increase of the overall temperature difference. The stress in the upper part shows little variation along the longitudinal position, while the stress in the lower part gradually decreases along the longitudinal position.

5. Conclusions

By conducting a sensitivity analysis on the parameter errors of the main bridge of Jinzhou Bridge, the extent of influence of relevant parameters has been determined, providing a theoretical basis and guidance for the construction control of the structure in the next phase.

1. It can be observed that the horizontal displacement of the bridge tower varies within the range of −0.6 mm to 0.6 mm when the stiffness of the main beam is increased or decreased by 5%. This indicates that the stiffness of the main beam has a minimal impact on the horizontal displacement of the bridge tower.
2. With a 2% increase in cable tension, the displacement increment is 3.8 mm, while with a 5% increase in cable tension, the displacement increment is 9.4 mm, causing the cable tower to shift towards the abutment. When the cable tension increases or decreases by the same percentage, the horizontal displacement change of the cable tower remains virtually the same, indicating that cable tension errors have a symmetric influence on the horizontal displacement of the cable tower.
3. It can be seen that the horizontal displacement variation of the tower caused by a temperature increase of 20°C and a temperature decrease of 20°C has reached −12.6 mm to 12.6 mm. The horizontal displacement variation of the tower increases with the increase of the temperature difference.

References

[1] H. Hao and E.K.C. Tang, “Numerical simulation of a cable-stayed bridge response to blast loads, Part II: Damage prediction and FRP strengthening”, *Engineering Structures*, vol. 32, no. 10, pp. 3193–3205, 2010, doi: 10.1016/j.engstruct.2010.06.006.

[2] X. Zheng and Y. Cui, "Analysis of static performance of cable-stayed arch cooperative bridge without back cable", *Archives of Civil Engineering*, vol. 62, no. 2, 2022, doi: 10.24425/ace.2022.140657.

[3] X. Shao, H. Zhao, and L. Li, "Design and experimental study of a harp-shaped single span cable-stayed bridge", *Journal of Bridge Engineering*, vol. 10, no. 6, pp. 658–665, 2005, doi: 10.1061/(ASCE)1084-0702(2005)10:6(658).

[4] T.C. Huynh, J.H. Park, and J.T. Kim, "Structural identification of cable-stayed bridge under back-to-back typhoons by wireless vibration monitoring", *Measurement*, vol. 88, pp. 385–401, 2016, doi: 10.1016/j.measurement.2016.03.032.

[5] Q. Han, J. Wen, X. Du, et al., "Nonlinear seismic response of a base isolated single pylon cable-stayed bridge", *Engineering Structures*, vol. 175, pp. 806–821, 2018, doi: 10.1016/j.engstruct.2018.08.077.

[6] F. Casciati, G.P. Cimellaro, and M. Domaneschi, "Seismic reliability of a cable-stayed bridge retrofitted with hysteretic devices", *Computers and Structures*, vol. 86, no. 17–18, pp. 1769–1781, 2008, doi: 10.1016/j.compstruc.2008.01.012.

[7] Y. Zhang, Z. Fang, R. Jiang, et al., "Static performance of a long-span concrete cable-stayed bridge subjected to multiple-cable loss during construction", *Journal of Bridge Engineering*, vol. 25, no. 3, 2020, doi: 10.1061/(ASCE)BE.1943-5592.0001529.

[8] H. Duan, H. Liu, Y. Sun, and H. Gao, "Determination of reasonable internal force state for cable-stayed bridge without backstays", *Journal of Civil Structural Health Monitoring*, vol. 13, pp. 1243–1263, 2023, doi: 10.1007/s13349-023-00706-4.

[9] A. Pipinato, C. Pellegrino, and C. Modena, "Structural analysis of the cantilever construction process in cable-stayed bridges", *Periodica Polytechnica. Civil Engineering*, vol. 56, no. 2, pp. 1–26, 2012, doi: 10.3311/pp.ci.2012-2.02.

[10] X. Sheng, W. Zheng, Z. Zhu, et al., "Ganjiang Bridge: A high-speed railway long-span cable-stayed bridge laying ballastless tracks", *Structural Engineering International*, vol. 31, no. 1, pp. 40–44, 2021, doi: 10.1080/10168664.2019.1671157.

[11] J. Farré-Checa, S. Komarizadehasl, H. Ma, et al., "Direct simulation of the tensioning process of cable-stayed bridge cantilever construction", *Automation in Construction*, vol. 137, art. no. 104197, 2022, doi: 10.1016/j.autcon.2022.104197.

[12] F. Xu, X. Wang, and L. Wang, "Cable inspection robot for cable-stayed bridges: Design, analysis, and application", *Journal of Field Robotics*, vol. 28, no. 3, pp. 441–459, 2011, doi: 10.1002/rob.20390.

[13] Z. Wang, B. He, Y. Zhou, et al., "Design and implementation of a cable inspection robot for cable-stayed bridges", *Robotica*, vol. 39, no. 8, pp. 1417–1433, 2021, doi: 10.1017/S0263574720001253.

[14] S. Cho, J. Yim, S.W. Shin, et al., "Comparative field study of cable tension measurement for a cable-stayed bridge", *Journal of Bridge Engineering*, vol. 18, no. 8, pp. 748–757, 2013, doi: 10.1061/(ASCE)BE.1943-5592.0000421.

[15] J. Zhang and F.T.K. Au, "Calibration of initial cable forces in cable-stayed bridge based on Kriging approach", *Finite Elements in Analysis and Design*, vol. 92, pp. 80–92, 2014, doi: 10.1016/j.finel.2014.08.007

Received: 2024-03-19, Revised: 2024-03-26